Strong thermal leptogenesis and the absolute neutrino mass scale

Pasquale Di Bari, Sophie E. King and Michele Re Fiorentin

School of Physics and Astronomy, University of Southampton,
Southampton, SO17 1BJ U.K.

E-mail: pdb1d08@soton.ac.uk, sk1806@soton.ac.uk, m.re-fiorentin@soton.ac.uk

Abstract. We show that successful strong thermal leptogenesis, where the final asymmetry is independent of the initial conditions and in particular a large pre-existing asymmetry is efficiently washed-out, favours values of the lightest neutrino mass $m_1 \gtrsim 10\,\text{meV}$ for normal ordering (NO) and $m_1 \gtrsim 3\,\text{meV}$ for inverted ordering (IO) for models with orthogonal matrix entries respecting $|\Omega_{ij}^2| \lesssim 2$. We show analytically why lower values of m_1 require a higher level of fine tuning in the seesaw formula and/or in the flavoured decay parameters (in the electronic for NO, in the muonic for IO). We also show how this constraint exists thanks to the measured values of the neutrino mixing angles and could be tightened by a future determination of the Dirac phase. Our analysis also allows us to place a more stringent constraint for a specific model or class of models, such as SO(10)-inspired models, and shows that some models cannot realise strong thermal leptogenesis for any value of m_1. A scatter plot analysis fully supports the analytical results. We also briefly discuss the interplay with absolute neutrino mass scale experiments concluding that they will be able in the coming years to either corner strong thermal leptogenesis or find positive signals pointing to a non-vanishing m_1. Since the constraint is much stronger for NO than for IO, it is very important that new data from planned neutrino oscillation experiments will be able to solve the ambiguity.

Keywords: leptogenesis, neutrino masses from cosmology

ArXiv ePrint: 1401.6185

Contents

1 Introduction

The observed matter-antimatter asymmetry of the Universe is a long standing cosmological puzzle calling for physics beyond the Standard Model (SM). In terms of the baryon-to-photon number ratio η_B the matter-antimatter asymmetry is today accurately and precisely measured by CMB observations. Recently the *Planck* collaboration found from CMB anisotropies plus lensing data[1] [1]

$$\eta_B^{\mathrm{CMB}} = (6.1 \pm 0.1) \times 10^{-10}. \tag{1.1}$$

Leptogenesis [2] provides an attractive solution since it relies on a minimal and natural way to extend the SM incorporating neutrino masses and mixing discovered in neutrino oscillation experiments: the seesaw mechanism [3–8]. At the same time it should be noticed that leptogenesis also relies on the Brout-Englert-Higgs mechanism and, therefore, the recent discovery of the Higgs boson at the LHC nicely contributes to support the picture. On the other hand the non-observation of new physics at the LHC so far, places stronger constraints on low scale baryogenesis scenarios such as, for example, electroweak baryogenesis within the minimal supersymmetric standard model [9–11].

The prediction of the baryon asymmetry relies on some assumption on the initial conditions. A plausible and common one is that an inflationary stage before leptogenesis resets the initial conditions in the early Universe, enforcing vanishing values of the asymmetry and

---

[1]More precisely the Planck collaboration finds $\Omega_B\, h^2 = 0.02217 \pm 0.00033$ corresponding to $10^{10}\,\eta_B \simeq 273.6\,\Omega_B\, h^2 \simeq 6.065 \pm 0.09$.

of the right-handed (RH) neutrino abundances prior to the onset of leptogenesis. However, it cannot be excluded, especially at the high temperatures required by a minimal scenario of leptogenesis [12], that other mechanisms, such as gravitational [13, 14], GUT [15–19], Affleck-Dine baryogenesis [20], generate a large asymmetry at the end of inflation and/or prior to the onset of leptogenesis.

Since these mechanisms escape experimental probes, it would be certainly more attractive if the final asymmetry from leptogenesis were independent of the initial conditions. In this paper we show that, given the current low energy neutrino data, the possibility to enforce independence of the initial conditions in leptogenesis, so called strong thermal leptogenesis, barring quasi-degenerate RH neutrino masses and strong fine tuned cancellations in the flavoured decay parameters and in the seesaw formula, implies a lower bound on the absolute neutrino mass scale, more specifically on the lightest neutrino mass. Though this lower bound can be evaded allowing for fine tuned cancellations, most of the models require values of the lightest neutrino mass that will be tested during the coming years, especially in the case of NO.

The plan of the paper is the following. In section 2 we introduce some basic notation and review current experimental information on low energy neutrino parameters. In section 3 we briefly discuss strong thermal leptogenesis. In section 4 we show the existence of a lower bound on the neutrino masses under certain conditions. We also present results from a scatter plot analysis confirming the existence of the lower bound and at the same time showing how the bulk of models require values of the lightest neutrino mass that can be potentially tested in future years mainly with cosmological observations. In section 5 we draw the conclusions.

2 General set up

We assume a minimal model of leptogenesis where the SM Lagrangian is extended introducing three RH neutrinos N_i with Yukawa couplings h and a Majorana mass term M. After spontaneous symmetry breaking the Higgs vev generates a Dirac neutrino mass term m_D. In the seesaw limit the spectrum of neutrino masses splits into a set of three heavy neutrinos with masses $M_1 \leq M_2 \leq M_3$, approximately equal to the eigenvalues of M, and into a set of light neutrinos with masses $m_1 \leq m_2 \leq m_3$ given by the seesaw formula

$$D_m = U^\dagger \, m_D \, \frac{1}{D_M} \, m_D^T \, U^\star \,, \tag{2.1}$$

written in a basis where both the Majorana mass and the charged lepton mass matrices are diagonal, so that U can be identified with the PMNS leptonic mixing matrix.

From neutrino oscillation experiments we know two mass squared differences, $\Delta m_{\rm atm}^2$ and $\Delta m_{\rm sol}^2$. Neutrino masses can then be either NO, with $m_3^2 - m_2^2 = \Delta m_{\rm atm}^2$ and $m_2^2 - m_1^2 = \Delta m_{\rm sol}^2$, or IO, with $m_3^2 - m_2^2 = \Delta m_{\rm sol}^2$ and $m_2^2 - m_1^2 = \Delta m_{\rm atm}^2$. For example, in a recent global analysis [21], and analogously in [22, 23], it is found $m_{\rm atm} \equiv \sqrt{m_3^2 - m_1^2} \simeq 0.0505\,(0.0493)\,{\rm eV}$ and $m_{\rm sol} \equiv \sqrt{\Delta m_{\rm sol}^2} \simeq 0.0087\,{\rm eV}$.

In order to fix completely the three light neutrino masses, there is just one parameter left to be measured, the so called absolute neutrino mass scale. This can be conveniently parameterised in terms of the lightest neutrino mass m_1. The most stringent upper bound on m_1 comes from cosmological observations. A conservative upper bound on the sum of the neutrino masses has been recently placed by the *Planck* collaboration [1]. Combining *Planck* and high-ℓ CMB anisotropies, WMAP polarisation and baryon acoustic oscillation data, it

is found $\sum_i m_i \lesssim 0.23\,\mathrm{eV}$ (95%C.L.). When neutrino oscillation results are combined, this translates into an upper bound on the lightest neutrino mass,

$$m_1 \lesssim 0.07\,\mathrm{eV} \quad (95\%\,\mathrm{C.L.})\,, \tag{2.2}$$

showing how cosmological observations start to corner quasi-degenerate neutrinos.

For NO the leptonic mixing matrix can be parameterised as

$$U^{(\mathrm{NO})} = \begin{pmatrix} c_{12}\,c_{13} & s_{12}\,c_{13} & s_{13}\,e^{-\mathrm{i}\delta} \\ -s_{12}\,c_{23} - c_{12}\,s_{23}\,s_{13}\,e^{\mathrm{i}\delta} & c_{12}\,c_{23} - s_{12}\,s_{23}\,s_{13}\,e^{\mathrm{i}\delta} & s_{23}\,c_{13} \\ s_{12}\,s_{23} - c_{12}\,c_{23}\,s_{13}\,e^{\mathrm{i}\delta} & -c_{12}\,s_{23} - s_{12}\,c_{23}\,s_{13}\,e^{\mathrm{i}\delta} & c_{23}\,c_{13} \end{pmatrix} \mathrm{diag}\left(e^{\mathrm{i}\,\rho}, 1, e^{\mathrm{i}\,\sigma}\right)\,, \tag{2.3}$$

$(s_{ij} \equiv \sin\theta_{ij}, c_{ij} \equiv \cos\theta_{ij})$ while for IO, within our convention of labelling light neutrino masses, the columns of the leptonic mixing matrix have to be permuted in a way that

$$U^{(\mathrm{IO})} = \begin{pmatrix} s_{13}\,e^{-\mathrm{i}\delta} & c_{12}\,c_{13} & s_{12}\,c_{13} \\ s_{23}\,c_{13} & -s_{12}\,c_{23} - c_{12}\,s_{23}\,s_{13}\,e^{\mathrm{i}\delta} & c_{12}\,c_{23} - s_{12}\,s_{23}\,s_{13}\,e^{\mathrm{i}\delta} \\ c_{23}\,c_{13} & s_{12}\,s_{23} - c_{12}\,c_{23}\,s_{13}\,e^{\mathrm{i}\delta} & -c_{12}\,c_{23} - s_{12}\,c_{23}\,s_{13}\,e^{\mathrm{i}\delta} \end{pmatrix} \mathrm{diag}\left(e^{\mathrm{i}\sigma}, e^{\mathrm{i}\,\rho}, 1\right)\,. \tag{2.4}$$

The mixing angles, respectively the reactor, the solar and the atmospheric one, are now constrained within the following 1σ (3σ) ranges [22] for NO and IO respectively,

$$s_{13}^2 = 0.0234_{-0.0018}^{+0.0022} \ \ (0.0177\text{–}0.0297) \ \text{ and } \ s_{13}^2 = 0.0239_{-0.0021}^{+0.0021} \ \ (0.0178\text{–}0.0300)\,, \tag{2.5}$$

$$s_{12}^2 = 0.308 \pm 0.017 \ \ (0.259\text{–}0.359) \ \text{ and } \ s_{12}^2 = 0.308 \pm 0.017 \ \ (0.259\text{–}0.359)\,,$$

$$s_{23}^2 = 0.425_{-0.027}^{+0.029} \ \ (0.357\text{–}0.641) \ \text{ and } \ s_{23}^2 = 0.437_{-0.029}^{+0.059} \oplus 0.531\text{–}0.610 \ \ (0.363\text{–}0.659)\,.$$

It is interesting that current experimental data also start to put constraints on the Dirac phase and the following best fit values and 1σ errors are found for NO and IO respectively,

$$\delta/\pi = -0.61_{-0.27}^{+0.33} \ \text{ and } \ \delta/\pi = -0.65_{-0.39}^{+0.24}\,, \tag{2.6}$$

while all values $[-\pi, +\pi]$ are still allowed at $3\,\sigma$.[2]

3   Strong thermal leptogenesis and the N_2-dominated scenario

Within an unflavoured scenario and assuming, conservatively, that only the lightest RH neutrinos thermalise, the strong thermal condition translates quite straightforwardly into a condition on the lightest RH neutrino decay parameter $K_1 \equiv \widetilde{\Gamma}_1/H(T = M_1)$, where H is the expansion rate and $\widetilde{\Gamma}_1$ is the N_1 total decay width. Given a pre-existing asymmetry $N_{B-L}^{\mathrm{p,i}}$, the relic value after the lightest RH neutrino wash-out is simply given by [2, 24]

$$N_{B-L}^{\mathrm{p,f}} = e^{-\frac{3\pi}{8}\,K_1}\,N_{B-L}^{\mathrm{p,i}}\,, \tag{3.1}$$

---

[2]It is also useful to give the constraints on the angles and on δ in degrees:

$$\theta_{13} = 8.8^\circ \pm 0.4^\circ \ \ (7.6^\circ\text{–}9.9^\circ) \ \text{ and } \ \theta_{13} = 8.9^\circ \pm 0.4^\circ \ \ (7.7^\circ\text{–}10^\circ)\,, \tag{2.7}$$

$$\theta_{12} = 33.70^\circ \pm 1.05^\circ \ \ (30.6^\circ\text{–}36.8^\circ) \ \text{ and } \ \theta_{12} = 33.7^\circ \pm 1.1^\circ \ \ (30.6^\circ\text{–}36.8^\circ)\,,$$

$$\theta_{23} = 40.7^\circ \pm 1.6^\circ \ \ (36.7^\circ\text{–}53.2^\circ) \ \text{ and } \ \theta_{23} = 41.4^{\circ\,+3.4^\circ}_{\ -1.8^\circ} \oplus 46.8^\circ\text{–}51.3^\circ \ \ (37^\circ\text{–}54.3^\circ)\,,$$

$$\delta = -110^{\circ\,+59^\circ}_{\ -49^\circ} \ \text{ and } \ \delta = -117^{\circ\,+43^\circ}_{\ -70^\circ}\,.$$

where we are indicating with N_X the abundance of any (extensive) quantity X in a co-moving volume containing one RH neutrino in ultra-relativistic thermal equilibrium (so that $N_{N_1}^{\text{eq}}(T \gg M_1) = 1$). The relic value of the pre-existing asymmetry would then result in a contribution to η_B given by $\eta_B^{\text{p}} \simeq 0.01 \, N_{B-L}^{\text{p,f}}$, taking into account the dilution due to photon production and the sphaleron conversion coefficient.

Imposing $|\eta_B^{\text{p}}| \lesssim 0.1 \, \eta_B^{\text{lep}} \simeq 0.1 \, \eta_B^{\text{CMB}}$, where η_B^{lep} is the contribution coming from leptogenesis, immediately yields the simple condition $K_1 \gtrsim K_{\text{st}}(N_{B-L}^{\text{p,i}})$, with

$$K_{\text{st}}(x) \equiv \frac{8}{3\pi} \left[\ln \left(\frac{0.1}{\eta_B^{\text{CMB}}} \right) + \ln |x| \right] \simeq 16 + 0.85 \ln |x| \,, \tag{3.2}$$

where $|N_{B-L}^{\text{p,i}}|$ is assumed to be large, meaning that $|N_{B-L}^{\text{p,i}}| \gg 100 \, \eta_B^{\text{CMB}} \sim 10^{-7}$. Since $K_1 \geq m_1/m_\star$, where $m_\star \simeq 1.1 \times 10^{-3}$ eV, the requirement $m_1 \gtrsim 10^{-3} \, K_{\text{st}}$ eV is a sufficient (but not necessary) condition for strong thermal leptogenesis.

When flavour effects are considered, the possibility to satisfy both successful leptogenesis, $\eta_B^{\text{lep}} \simeq \eta_B^{\text{CMB}}$, and strong thermal condition, $|\eta_B^{\text{p}}| \lesssim 0.1 \, \eta_B^{\text{lep}}$, relies on much more restrictive conditions [25], due to the 3-dim flavour space and to the fact that the RH neutrino wash-out acts only along a specific flavour component [26, 27].

It is then possible to show [25] that only in a N_2-*dominated scenario* [28], defined by having $M_1 \ll 10^9$ GeV and $M_2 \gtrsim 10^9$ GeV, so that the observed asymmetry is dominantly produced by the N_2 RH neutrinos, with the additional requirements $M_2 \lesssim 5 \times 10^{11}$ GeV,[3] and that the asymmetry is dominantly produced in the tauon flavour, one can have successful strong thermal leptogenesis.

In the N_2-dominated scenario the contribution to the asymmetry from leptogenesis can be calculated as the sum of the three (charged lepton) flavoured asymmetries $\Delta_\alpha \equiv B/3 - L_\alpha$, [34–38]

$$
\begin{aligned}
N_{B-L}^{\text{lep,f}} \simeq &\left[\frac{K_{2e}}{K_{2\tau_2^\perp}} \varepsilon_{2\tau_2^\perp} \kappa\left(K_{2\tau_2^\perp}\right) + \left(\varepsilon_{2e} - \frac{K_{2e}}{K_{2\tau_2^\perp}} \varepsilon_{2\tau_2^\perp} \right) \kappa\left(K_{2\tau_2^\perp}/2\right) \right] e^{-\frac{3\pi}{8} K_{1e}} + \\
&+ \left[\frac{K_{2\mu}}{K_{2\tau_2^\perp}} \varepsilon_{2\tau_2^\perp} \kappa\left(K_{2\tau_2^\perp}\right) + \left(\varepsilon_{2\mu} - \frac{K_{2\mu}}{K_{2\tau_2^\perp}} \varepsilon_{2\tau_2^\perp} \right) \kappa\left(K_{2\tau_2^\perp}/2\right) \right] e^{-\frac{3\pi}{8} K_{1\mu}} + \\
&+ \varepsilon_{2\tau} \, \kappa(K_{2\tau}) \, e^{-\frac{3\pi}{8} K_{1\tau}} \,,
\end{aligned}
\tag{3.3}
$$

where $K_{2\tau_2^\perp} \equiv K_{2e} + K_{2\mu}$ and $\varepsilon_{2\tau_2^\perp} \equiv \varepsilon_{2e} + \varepsilon_{2\mu}$. As we will show soon, the strong thermal condition implies $K_{1e}, K_{1\mu} \gg 1$ and, therefore, in this case the contribution to the asymmetry from leptogenesis simply reduces to

$$N_{B-L}^{\text{lep,f}} \simeq \varepsilon_{2\tau} \, \kappa(K_{2\tau}) \, e^{-\frac{3\pi}{8} K_{1\tau}} \,. \tag{3.4}$$

The baryon-to-photon number ratio from leptogenesis can then be simply calculated as $\eta_B^{\text{lep}} \simeq 0.01 \, N_{B-L}^{\text{lep,f}}$. The flavoured decay parameters $K_{i\alpha}$ are defined as

$$K_{i\alpha} \equiv \frac{\Gamma_{i\alpha} + \overline{\Gamma}_{i\alpha}}{H(T = M_i)} = \frac{|m_{D\alpha i}|^2}{M_i \, m_\star} \,. \tag{3.5}$$

---

[3]In this way the asymmetry production from N_2 decays occurs in the two-flavour regime [26, 27, 29–33].

The $\Gamma_{i\alpha}$'s and the $\bar{\Gamma}_{i\alpha}$'s can be regarded as the zero temperature limit of the flavoured decay rates into α leptons, $\Gamma(N_i \to \phi^\dagger l_\alpha)$, and anti-leptons, $\Gamma(N_i \to \phi \bar{l}_\alpha)$ in a three-flavoured regime, where lepton quantum states can be treated as an incoherent mixture of the three flavour components. They are related to the total decay widths by $\widetilde{\Gamma}_i = \sum_\alpha \widetilde{\Gamma}_{i\alpha}$, with $\widetilde{\Gamma}_{i\alpha} \equiv \Gamma_{i\alpha} + \bar{\Gamma}_{i\alpha}$. The efficiency factors can be calculated using [39, 40]

$$\kappa(K_{2\alpha}) = \frac{2}{z_B(K_{2\alpha})\, K_{2\alpha}} \left(1 - e^{-\frac{K_{2\alpha}\, z_B(K_{2\alpha})}{2}}\right), \qquad z_B(K_{2\alpha}) \simeq 2 + 4\, K_{2\alpha}^{0.13}\, e^{-\frac{2.5}{K_{2\alpha}}}. \quad (3.6)$$

This is the expression for an initial thermal abundance but, since we will impose the strong thermal leptogenesis condition, this will automatically select the region of the space of parameters where there is no dependence on the initial conditions anyway.[4]

Within the N_2-dominated scenario the flavoured CP asymmetries, defined as $\varepsilon_{2\alpha} \equiv (\bar{\Gamma}_{2\alpha} - \Gamma_{2\alpha})/(\Gamma_{2\alpha} + \bar{\Gamma}_{2\alpha})$, can be calculated in the hierarchical limit simply using [41]

$$\varepsilon_{2\alpha} \simeq \bar{\varepsilon}(M_2)\, \beta_{2\alpha}, \qquad \beta_{2\alpha} \equiv \frac{\mathrm{Im}\left[m_{D\alpha2}^\star m_{D\alpha3}(m_D^\dagger\, m_D)_{23}\right]}{M_2\, M_3\, \widetilde{m}_2\, m_{\mathrm{atm}}}, \quad (3.7)$$

with $\widetilde{m}_2 \equiv (m_D^\dagger\, m_D)_{22}/M_2$ and $\bar{\varepsilon}(M_2) \equiv [3/(16\,\pi)]\,(M_2\, m_{\mathrm{atm}}/v^2)$.

In the orthogonal parameterisation the neutrino Dirac mass matrix, in the basis where both charged lepton and RH neutrino mass matrices are diagonal, can be written as $m_D = U\,\sqrt{D_m}\,\Omega\,\sqrt{D_M}$, where Ω is an orthogonal matrix encoding the information on the properties of the RH neutrinos [42]. This parameterisation is quite convenient in order to easily account for the experimental low energy neutrino information. Barring strong cancellations in the seesaw formula, one typically expects $|\Omega_{ij}^2| \lesssim \mathcal{O}(1)$. More generally, we will impose a condition $|\Omega_{ij}^2| < M_\Omega$, studying the dependence of the results on M_Ω. In the orthogonal parametrisation the flavoured decay parameters can be calculated as

$$K_{i\alpha} = \left|\sum_j \sqrt{\frac{m_j}{m_\star}}\, U_{\alpha j}\, \Omega_{ji}\right|^2. \quad (3.8)$$

The quantity $\beta_{2\alpha}$ can also be expressed in the orthogonal parameterisation,

$$\beta_{2\alpha} = \mathrm{Im}\left[\sum_{k,h,l} \frac{m_k\, \sqrt{m_h\, m_l}}{\widetilde{m}_2\, m_{\mathrm{atm}}}\, \Omega_{k2}^*\, \Omega_{k3}\, \Omega_{h2}^*\, \Omega_{l3}\, U_{\alpha h}^*\, U_{\alpha l}\right]. \quad (3.9)$$

Now, we have finally to impose the strong thermal condition, and to this extent we need to calculate the relic value of the pre-existing asymmetry distinguishing two different cases.

3.1 Case $M_3 \gtrsim 5 \times 10^{11}\,\mathrm{GeV}$

In the case $M_3 \gtrsim 5 \times 10^{11}\,\mathrm{GeV}$, the heaviest RH neutrino either, for $M_3 \gg T_{RH}$, is not thermalised or it cannot in general wash-out completely the pre-existing asymmetry, as requested by the strong thermal leptogenesis condition. This is because the wash-out would occur in the one-flavour regime and, for a generic pre-existing asymmetry, the component orthogonal to the N_3-flavour direction would survive. Therefore, without any loss of generality, we

---

[4]Moreover in this case this analytical expression approximates the numerical result with an error below 10%.

can simply neglect its presence. The relic value of the pre-existing asymmetry can then be calculated as [43] $N_{B-L}^{\mathrm{p,f}} = \sum_\alpha N_{\Delta_\alpha}^{\mathrm{p,f}}$, with

$$N_{\Delta_\tau}^{\mathrm{p,f}} = \left(p_{\mathrm{p}\tau}^0 + \Delta p_{\mathrm{p}\tau}\right) e^{-\frac{3\pi}{8}(K_{1\tau}+K_{2\tau})} N_{B-L}^{\mathrm{p,i}}, \tag{3.10}$$

$$N_{\Delta_\mu}^{\mathrm{p,f}} = \left\{\left(1 - p_{\mathrm{p}\tau}^0\right)\left[p_{\mu\tau_2^\perp}^0 p_{\mathrm{p}\tau_2^\perp}^0 e^{-\frac{3\pi}{8}(K_{2e}+K_{2\mu})} + \left(1 - p_{\mu\tau_2^\perp}^0\right)\left(1 - p_{\mathrm{p}\tau_2^\perp}^0\right)\right] + \Delta p_{\mathrm{p}\mu}\right\} e^{-\frac{3\pi}{8}K_{1\mu}} N_{B-L}^{\mathrm{p,i}},$$

$$N_{\Delta_e}^{\mathrm{p,f}} = \left\{\left(1 - p_{\mathrm{p}\tau}^0\right)\left[p_{e\tau_2^\perp}^0 p_{\mathrm{p}\tau_2^\perp}^0 e^{-\frac{3\pi}{8}(K_{2e}+K_{2\mu})} + \left(1 - p_{e\tau_2^\perp}^0\right)\left(1 - p_{\mathrm{p}\tau_2^\perp}^0\right)\right] + \Delta p_{\mathrm{pe}}\right\} e^{-\frac{3\pi}{8}K_{1e}} N_{B-L}^{\mathrm{p,i}}.$$

In this expression[5] the quantities $p_{\mathrm{p}\tau}^0$ and $p_{\mathrm{p}\tau_2^\perp}^0$ are the fractions of the pre-existing asymmetry in the tauon and $\tau_2^\perp$ components respectively, where $\tau_2^\perp$ is the τ-orthogonal flavour component of the leptons produced by N_2 decays, while $p_{\alpha\tau_2^\perp}^0 \equiv K_{2\alpha}/(K_{2e}+K_{2\mu})$ $(\alpha = e, \mu)$ is the fraction of α-asymmetry that is first washed-out by the N_2 inverse processes in the tauon-orthogonal plane and then by the N_1 inverse processes.

The terms Δp_{pe}, $\Delta p_{\mathrm{p}\mu}$ and $\Delta p_{\mathrm{p}\tau}$, with $\Delta p_{\mathrm{pe}} + \Delta p_{\mathrm{p}\mu} + \Delta p_{\mathrm{p}\tau} = 0$, take into account the possibility of different flavour compositions of the pre-existing leptons and anti-leptons. This would lead to initial values of the pre-existing α asymmetries that are not necessarily just a fraction of $N_{B-L}^{\mathrm{p,i}}$. The presence of these terms depends on the specific mechanism that produced the pre-existing asymmetry. For example in leptogenesis itself they are in general present, they are the so called phantom terms. However, this indefiniteness has just a very small effect on the results. If the $\Delta p_{\mathrm{p}\alpha}$-terms are not present, then in principle very special flavour configurations with $1 - p_{e\tau_2^\perp}^0, 1 - p_{\mu\tau_2^\perp}^0 \ll 1$ could also lead to a wash-out of the pre-existing asymmetries without the need to impose $K_{1e}, K_{1\mu} \gg 1$. We will comment on this possibility but for the time being we will assume that these terms are present. In this case the condition of successful strong thermal leptogenesis translates into the straightforward set of conditions

$$K_{1e}, K_{1\mu} \gtrsim K_{\mathrm{st}}(N_{\Delta_{e,\mu}}^{\mathrm{p,i}}), \qquad K_{2\tau} \gtrsim K_{\mathrm{st}}(N_{\Delta_\tau}^{\mathrm{p,i}}), \qquad K_{1\tau} \lesssim 1. \tag{3.11}$$

These conditions guarantee a washout of the electron and muon asymmetries, only possible in the three-flavoured regime at $T \ll 10^9\,\mathrm{GeV}$, and at the same time also a wash-out of the tauon asymmetry in the two-flavoured regime. The latter is still compatible with a generation of a sizeable tauon asymmetry from N_2 decays. This is the only possibility [25]. It should be noticed that in the N_2-dominated scenario the existence of the heaviest RH neutrino N_3 is necessary in order to have an interference of tree level N_2 decays with one-loop N_2 decay graphs containing virtual N_3 yielding sufficiently large $\varepsilon_{2\alpha}$. Therefore, within the N_2-dominated scenario, where by definition $M_1 \ll 10^9\,\mathrm{GeV}$, one has a phenomenological reason to have at least three RH neutrino species [28].[6]

---

[5]Notice that in the limit $K_{1\alpha} = K_{2\alpha} = 0$ $(\alpha = e, \mu, \tau)$ one has $\sum_\alpha N_{\Delta_\alpha}^{\mathrm{p,f}} = N_{B-L}^{\mathrm{p,i}}$. Notice also that this expression incorporates flavour projection [26, 27] and exponential suppression of the parallel components, two effects that have been both confirmed within a density matrix approach [38].

[6]In the limit $M_3 \to \infty$, when N_3 decouples and a two RH neutrino scenario is effectively recovered with $m_1 = 0$, one has $\beta_{2\alpha} \to 0$ (cf. eq. (3.7)). In this limit the only possibility to realise successful leptogenesis is to have sizeable CP asymmetries from the interference terms with the lightest RH neutrinos that we neglected when we wrote eq. (3.7). These terms are $\propto M_1$ and successful leptogenesis necessarily requires in the end a lower bound $M_1 \gtrsim 2 \times 10^{10}\,\mathrm{GeV}$ [44]. However, then in this case the N_1-produced asymmetry not only cannot be neglected but typically dominates on the N_2-produced asymmetry and moreover, more importantly for us, strong thermal leptogenesis cannot be realised [25]. This well illustrates that in the N_2-dominated scenario, the presence of a (coupled) N_3 is necessary for successful leptogenesis.

3.2 Case $M_3 \lesssim 5 \times 10^{11}\,\mathrm{GeV}$

If $M_3 \lesssim 5 \times 10^{11}\,\mathrm{GeV}$, then the heaviest RH neutrinos N_3 can contribute to wash-out the tauon component together with the next-to-lightest RH neutrinos N_2. In this way, for the relic value of the pre-existing asymmetry, one obtains ($\alpha = e, \mu$)

$$N_{\Delta_\tau}^{\mathrm{p,f}} = (p_{\mathrm{p}\tau}^0 + \Delta p_{\mathrm{p}\tau}) e^{-\frac{3\pi}{8}(K_{1\tau}+K_{2\tau}+K_{3\tau})} N_{B-L}^{\mathrm{p,i}}, \tag{3.12}$$

$$N_{\Delta_\alpha}^{\mathrm{p,f}} = \left\{ \left(1 - p_{\mathrm{p}\tau}^0\right) \left[p_{\mathrm{p}\tau_3^\perp}^0 p_{\tau_3^\perp \tau_2^\perp}^0 p_{\tau_2^\perp \alpha}^0 e^{-\frac{3\pi}{8}\left(K_{3\tau^\perp}+K_{2\tau^\perp}\right)} + \left(1 - p_{\mathrm{p}\tau_3^\perp}^0\right) \left(1 - p_{\tau_3^\perp \tau_2^\perp}^0\right) p_{\tau_2^\perp \alpha}^0 e^{-\frac{3\pi}{8}K_{2\tau^\perp}} \right. \right.$$
$$\left. \left. + \; p_{\mathrm{p}\tau_3^\perp}^0 \left(1 - p_{\mathrm{p}\tau_2^\perp}^0\right) \left(1 - p_{\tau_2^\perp \alpha}^0\right) \right] + \Delta p_{\mathrm{p}\alpha} \right\} e^{-\frac{3\pi}{8}K_{1\alpha}} N_{B-L}^{\mathrm{p,i}},$$

where we defined $K_{2\tau^\perp} \equiv K_{2e} + K_{2\mu}$ and $K_{3\tau^\perp} \equiv K_{3e} + K_{3\mu}$. The inclusion of the N_3-washout relaxes the condition $K_{2\tau} \gg 1$ to $K_{2\tau} + K_{3\tau} \gg 1$. In this way one can have strong thermal leptogenesis with lower values of $K_{2\tau}$ and so the condition of successful leptogenesis can be more easily satisfied. Therefore, in this case the constraints from successful strong thermal leptogenesis could potentially get relaxed.

4 Lower bound on neutrino masses

In this section we show finally that the strong thermal condition implies, for sufficiently large pre-existing asymmetries and barring fine tuned conditions on the values of the flavour decay parameters and in the seesaw formula, the existence of a lower bound on the lightest neutrino mass and, more generally, a strong reduction of the accessible region of parameters for $m_1 \lesssim 10\,\mathrm{meV}$.

The main point is that the conditions $K_{1\tau} \lesssim 1$ and $K_{1e}, K_{1\mu} \gtrsim K_{\mathrm{st}} \gg 1$ can be satisfied simultaneously only for sufficiently large values of m_1.

4.1 Case $M_3 \gtrsim 5 \times 10^{11}\,\mathrm{GeV}$

Let us start discussing the more significant case $M_3 \gtrsim 5 \times 10^{11}\,\mathrm{GeV}$, when, as already pointed out, the N_3 wash-out can be neglected. The cases of NO and IO need also to be discussed separately. Let us start from NO.

4.1.1 NO neutrino masses

We want to show that the conditions $K_{1\tau} \lesssim 1$ and $K_{1e}, K_{1\mu} \gtrsim K_{\mathrm{st}} \gg 1$ can be satisfied simultaneously, without fine-tuned conditions, only if m_1 is sufficiently large. Let us start by analysing $K_{1\tau}$. The general eq. (3.8) for the $K_{i\alpha}$'s specialises into

$$K_{1\tau} = \left| \sqrt{\frac{m_1}{m_\star}} U_{\tau 1} \Omega_{11} + \sqrt{\frac{m_2}{m_\star}} U_{\tau 2} \Omega_{21} + \sqrt{\frac{m_3}{m_\star}} U_{\tau 3} \Omega_{31} \right|^2. \tag{4.1}$$

From this expression, anticipating that the lower bound falls into a range of values $m_1 \lesssim m_{\mathrm{sol}}$ so that we can approximate $m_2 \simeq m_{\mathrm{sol}}$ and $m_3 \simeq m_{\mathrm{atm}}$, we can write

$$\sqrt{\frac{m_{\mathrm{atm}}}{m_\star}} U_{\tau 3} \Omega_{31} = -\sqrt{\frac{m_1}{m_\star}} U_{\tau 1} \Omega_{11} - \sqrt{\frac{m_{\mathrm{sol}}}{m_\star}} U_{\tau 2} \Omega_{21} + \sqrt{K_{1\tau}}\, e^{i\varphi}, \tag{4.2}$$

where φ is some generic phase. If we now insert this expression into the expressions for K_{1e} and $K_{1\mu}$, we can impose ($\alpha = e, \mu$)

$$K_{1\alpha} = \left| \Omega_{11} \sqrt{\frac{m_1}{m_\star}} \left(U_{\alpha 1} - \frac{U_{\tau 1}}{U_{\tau 3}} U_{\alpha 3} \right) + \sqrt{K_{1\alpha}^0}\, e^{i\,\varphi_0} \right|^2 > K_{\mathrm{st}}(N_{\Delta_\alpha}^{\mathrm{p,i}}), \tag{4.3}$$
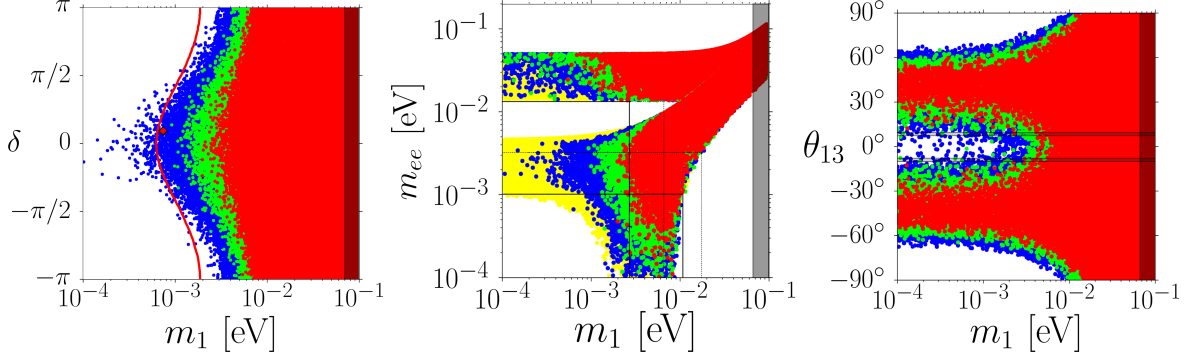
Figure 1. NO case. Scatter plot points in the planes $\delta - m_1$ (left), $m_{ee} - m_1$ (center), $\theta_{13} - m_1$ (right) satisfying successful strong thermal leptogenesis for $N_{B-L}^{\mathrm{p,i}} = 10^{-1}$ (red), 10^{-2} (green) and 10^{-3} (blu). In all panels the vertical gray band is the *Planck* m_1 upper bound eq. (2.2). In the left panel points are plotted for $M_\Omega = 2$ and the red solid line is the analytic lower bound $m_1^{\mathrm{lb}}(\delta)$ (cf. eq. (4.5)) for $N_{B-L}^{\mathrm{p,i}} = 10^{-1}$. While the points in the left and central panels have been obtained for uniform random values of the three mixing angles generated within the 3σ ranges eq. (2.5), in the right panel they have been left free (the horizontal band indicates the 3σ range in eq. (2.5) for θ_{13}). In the central panel the vertical lines indicate the m_1 values above which 99% of scatter plot points are found (see central panel in figure 4).

where we defined $K_{1\alpha}^0 \equiv K_{1\alpha}(m_1 = 0)$ and φ_0 such that

$$\sqrt{K_{1\alpha}^0}\, e^{i\varphi_0} \equiv \Omega_{21} \sqrt{\frac{m_{\mathrm{sol}}}{m_\star}} \left(U_{\alpha 2} - \frac{U_{\tau 2}}{U_{\tau 3}} U_{\alpha 3} \right) + \frac{U_{\alpha 3}}{U_{\tau 3}} \sqrt{K_{1\tau}}\, e^{i\varphi}\,. \tag{4.4}$$

From this condition one obtains a lower bound on m_1 ($\alpha = e, \mu$),

$$m_1 > m_1^{\mathrm{lb}} \equiv m_\star \max_\alpha \left[\left(\frac{\sqrt{K_{\mathrm{st}}} - \sqrt{K_{1\alpha}^{0,\mathrm{max}}}}{\max[|\Omega_{11}|] \left| U_{\alpha 1} - \frac{U_{\tau 1}}{U_{\tau 3}} U_{\alpha 3} \right|} \right)^2 \right] \tag{4.5}$$

when $K_{1\alpha}^{0,\mathrm{max}} < K_{\mathrm{st}}$, where we defined

$$K_{1\alpha}^{0,\mathrm{max}} \equiv \left(\max[|\Omega_{21}|] \sqrt{\frac{m_{\mathrm{sol}}}{m_\star}} \left| U_{\alpha 2} - \frac{U_{\tau 2}}{U_{\tau 3}} U_{\alpha 3} \right| + \left| \frac{U_{\alpha 3}}{U_{\tau 3}} \right| \sqrt{K_{1\tau}^{\mathrm{max}}} \right)^2 \,. \tag{4.6}$$

Because of the smallness of the reactor mixing angle θ_{13} there are two consequences: the first is that the maximum is found for $\alpha = e$ and the second is that, imposing $K_{1\tau}^{\mathrm{max}} \lesssim 1$, both the two terms in $K_{1e}^{0,\mathrm{max}}$ proportional to U_{e3} are suppressed and in this way there is indeed a lower bound for a sufficiently small value of $\max[|\Omega_{21}|]$.

In the left panel of figure 1 we have conservatively taken $\max[|\Omega_{21}^2|] = \max[|\Omega_{11}^2|] = M_\Omega = 2$ and plotted m_1^{lb} at 95% C.L. for $N_{B-L}^{\mathrm{p}} = 0.1$ as a function of the Dirac phase δ.[7]

---

[7]We used Gaussian ranges for the mixing angles within as in eq. (2.5), except for the atmospheric mixing angle for which we used a Gaussian distribution $s_{23}^2 = 0.5 \pm 0.1$, i.e. centred on the maximal mixing value since on this angle results are still unstable depending on the analysis. We have also used, in the scatter plot analysis as well, $p_{\mathrm{p}\tau_2^\perp}^0/2 = p_{\mathrm{p}\tau}^0 = \Delta p_{\mathrm{pe}} = \Delta p_{\mathrm{p}\mu} = 1/3$, corresponding to a flavour blind pre-existing asymmetry. Notice in any case that results depend only logarithmically on these parameters, so they are insensitive to a precise choice.
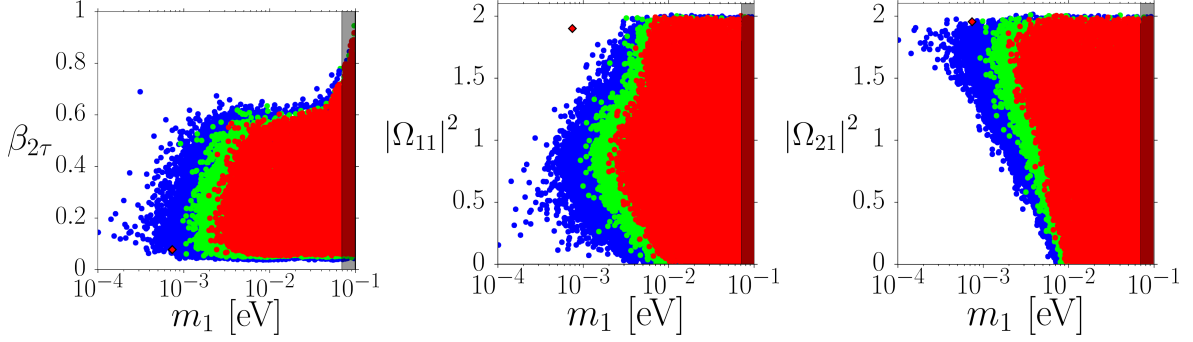
Figure 2. NO case. Results of the scatter plots for $M_\Omega = 2$ for $\beta_{2\tau} \equiv \varepsilon_{2\tau}/\bar{\varepsilon}(M_2)$, $|\Omega_{11}^2|$ and $|\Omega_{21}^2|$ versus m_1 (same colour code as in figure 1).

At $\delta = 0$ we find (top right panel) $m_1^{\rm lb} \simeq 0.7\,\mathrm{meV}$ while for $\delta = \pm\pi$ we obtain $m_1^{\rm lb} \simeq 2\,\mathrm{meV}$, showing how a future determination of the Dirac phase δ could tighten the lower bound. The lower bound becomes more stringent for $M_\Omega = 1$ and we find $m_1^{\rm lb}(\delta = 0) \simeq 6\,\mathrm{meV}$. On the other hand for $M_\Omega = 3$ the lower bound gets relaxed and we obtain $m_1^{\rm lb}(\delta = 0) \simeq 0.13\,\mathrm{meV}$. For $M_\Omega \gtrsim 4$ one can easily verify that the condition $K_{\rm st} > K_{1\alpha}^{0,\rm max}$ ($\alpha = e, \mu$) is not verified and there is no lower bound on m_1.

In order to verify the existence of the lower bound, to test the validity of the analytic estimation and to show in more detail the level of fine tuning involved in order to saturate the lower bound, we performed a scatter plot analysis in the space of the 13 parameters (m_1, 6 in U, 6 in Ω) for $M_\Omega = 1, 2, 5, 10$. The results are shown in figure 1. for three values of $N_{B-L}^{\rm p,i} = 10^{-1}, 10^{-2}, 10^{-3}$ (respectively the red, green and blue points). One can see that for $N_{B-L}^{\rm p,i} = 10^{-1}$ the minimum values of m_1 in the left panel at different values of δ are much higher than the analytic estimation (one has to compare the red points with the red solid line). The reason is due to the fact that the lower bound is saturated for very special choices of Ω such that $\max[|\Omega_{11}^2|], \max[|\Omega_{21}^2|]$ are as close as possible to the maximum value M_Ω without suppress the CP asymmetry $\varepsilon_{2\tau}$ needed to have successful leptogenesis. This is confirmed by figure 2 where in the three panels we have plotted $\beta_{2\tau} \equiv \varepsilon_{2\tau}/\bar{\varepsilon}(M_2)$, $|\Omega_{11}^2|$ and $|\Omega_{22}^2|$ for $M_\Omega = 2$. We have made a focused search (by fine-tuning the parameters) managing to find a point (the red diamond) where m_1 is very close to the lower bound. For this point $\beta_{2\tau}$ gets considerably reduced since it corresponds to a situation where the term $\propto \sqrt{m_1}$ in the flavoured decay parameters becomes negligible and the strong thermal condition is satisfied for a very special condition, basically the eq. (4.2) when the terms $\propto \sqrt{m_1}, \sqrt{K_{1\tau}}$ are neglected in the right-hand side and $|\Omega_{11}|, |\Omega_{21}|$ become maximal, that leads to a CP asymmetry suppression.

We have also performed a scatter plot letting the mixing angles to vary within the whole range of physical values with no experimental constraints. In the right panel of figure 1 we show the results in the plane $m_1 - \theta_{13}$. One can see how the smallness of θ_{13} is crucial for the existence of the lower bound. This can be well understood analytically considering that in the expression for $K_{1e}^{0,\rm max}$ there are two terms $\propto |U_{e3}|^2$ (cf. eq. (4.6)).

In figure 3 we also show the results for the values of the three $K_{1\alpha}$ ($\alpha = e, \mu, \tau$) and for $K_{2\tau}$, the four relevant flavoured decay parameters, for $M_\Omega = 2$. First of all one can see how the values of the flavoured decay parameters respect the strong thermal conditions eq. (3.11). However, the most important plot is that one for K_{1e}, showing how for values $m_1 \lesssim 10\,\mathrm{meV}$ the maximum value of K_{1e} gets considerably reduced until it falls below $K_{\rm st}$, indicated by the
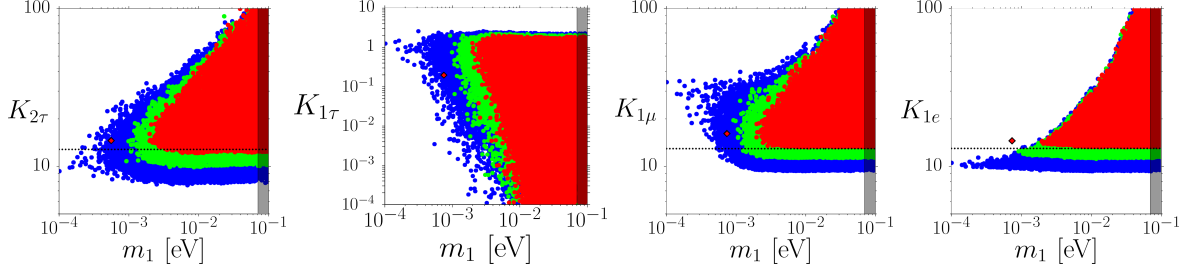
Figure 3. NO case. Results of the scatter plots for $M_\Omega = 2$ for the four relevant flavoured decay parameters $K_{2\tau}, K_{1\tau}, K_{1\mu}, K_{1e}$ versus m_1 (conventions as in figure 1). The horizontal dashed line indicates the value $K_{\rm st}(N_{\Delta_\alpha}^{\rm p,i} = 0.03) \simeq 13$ (cf. eq. (3.2)).
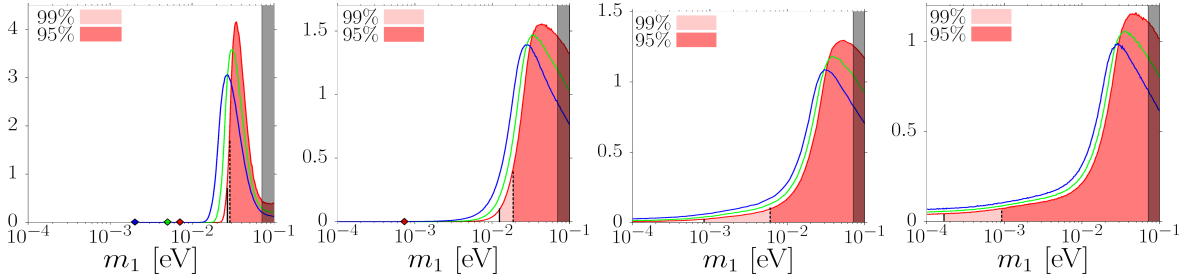

Figure 4. NO case. Distribution of probability of m_1 from the scatter plots for $M_\Omega = 1, 2, 5, 10$ from left to right for different values of $N_{B-L}^{\rm p,i}$ (same conventions as in figure 1). The diamonds mark the m_1 minimum value (if found).

horizontal dashed line for $N_{B-L}^{\rm p,i} = 0.1$, at the m_1 lower bound value (very closely realised by the red diamond point). It is also clear that already below $\sim 10\,{\rm meV}$ the possibility to realise strong thermal leptogenesis requires a high fine tuning in the parameters since in this case $K_{1e} \lesssim K_{1e}^{0,\rm max} \simeq 4\,M_\Omega \lesssim K_{\rm st}$ for large asymmetries and not too unreasonably high values of M_Ω. This is well illustrated in figure 4 where we plotted the distribution of the m_1 values from the scatter plots for $M_\Omega = 1, 2, 5, 10$ and for $N_{B-L}^{\rm p,i} = 10^{-1}, 10^{-2}, 10^{-3}$.

One can see that there is a clear peak around $m_1 \simeq m_{\rm atm}$. One can also see that the distributions rapidly tend to zero when $m_1 \lesssim m_{\rm sol} \simeq 10\,{\rm meV}$. For example, for our benchmark value $M_\Omega = 2$ and for $N_{B-L}^{\rm p,i} = 10^{-1}$, it can be noticed how more than 99% of points falls for values $m_1 \gtrsim 10\,{\rm meV}$ (the value quoted in the abstract). Even for $M_\Omega = 5$ one still has that the 95% of points satisfying successful strong thermal leptogenesis is found for $m_1 \gtrsim 6\,{\rm meV}$. It is also interesting to notice how this constraint gets only slightly relaxed for lower values of the pre-existing asymmetry. Only for $M_\Omega = 10$ one obtains that 95% of points fall at $m_1 \gtrsim 1\,{\rm meV}$. For $M_\Omega = 100$, not shown in the plots, this would decrease at (untestable) values $m_1 \gtrsim 0.4\,{\rm meV}$. This provides another example of how, more generally, leptogenesis neutrino mass bounds tend to disappear in the limit $M_\Omega \gg 1$ [45, 46]. It should be however said how large values of $|\Omega_{ij}^2|$ imply high cancellations in the see-saw formula such that the lightness of LH neutrinos becomes a combined effect of these cancellations with the the see-saw mechanism and they are typically not realised in models embedding a genuine minimal type I see-saw mechanism.

Clearly the results on the m_1 distributions in figure 4 depend on the orthogonal matrix parameterisation that we used in order to generate the points on the scatter plots but they
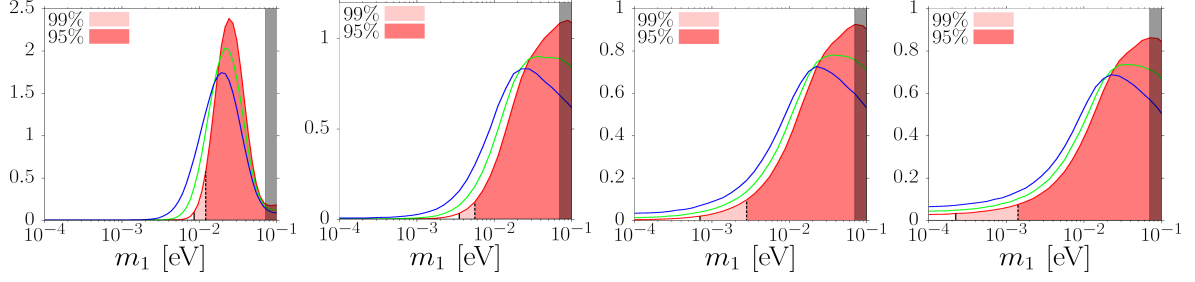
Figure 5. IO case. Density of probabilities of m_1 from the scatter plots for $M_\Omega = 1, 2, 5, 10$ from left to right (same conventions as in figure 1).

provide quite a useful indication of the level of fine tuning required to satisfy successful strong thermal leptogenesis for values of the lightest neutrino mass below $\sim 10\,\mathrm{meV}$. In any case it is fully explained by our analytical discussion and by the plot of the maximum of K_{1e} values that is independent of the specific parameterisation. We also double checked the results producing scatter plots for two different parameterisations. In a first case we used the usual parameterisation of the orthogonal matrix in terms of complex rotations described by three complex Euler angles, that, however, has the drawback not to be flavour blind. In a second case we used a parameterisation based on the isomorphism between the group of complex orthogonal matrices and the Lorentz group. We did not find any appreciable difference.[8]

4.1.2   IO neutrino masses

Let us now discuss the case of IO. The analytical procedure we have discussed for NO can be repeated in the IO case and one finds the same expression eq. (4.5) for the lower bound on m_1 where, however, one has to replace $m_{\mathrm{sol}} \to m_{\mathrm{atm}}$ and $U \to U^{(\mathrm{IO})}$.

The replacement $m_{\mathrm{sol}} \to m_{\mathrm{atm}}$ tends to push all $K_{1\alpha}$ values to much higher values and this is indeed what happens for K_{1e}. If one considers again the quantity $K_{1e}^{0,\mathrm{max}}$ (cf. eq. (4.6)) it is possible to check that this time one has always $K_{1e}^{0,\mathrm{max}} \gg K_{\mathrm{st}}$ for $N_{B-L}^{\mathrm{p,i}} \lesssim 0.1$. On the other hand this time the value of $K_{1\mu}$ has to be fine tuned in order to be greater than K_{st}. The reason is that for IO there is now a cancellation in the quantity $[U_{\mu2} - U_{\tau2}\, U_{\mu3}/U_{\tau3}]^{(\mathrm{IO})}$ that suppresses $K_{1\mu}^{0,\mathrm{max}}$ though not as strongly as $K_{1e}^{0,\mathrm{max}}$ in the NO case. Indeed one finds now that $K_{1\mu}^{0,\mathrm{max}} < K_{\mathrm{st}}$, the condition for the existence of the lower bound, holds only for $M_\Omega \lesssim 0.9$. This implies that the lower bound on m_1 for IO is much looser than for the NO case. This result is again confirmed by a scatter plot analysis. The results are shown in figure 5 directly in the form of the distribution of probabilities for m_1. One can see how this time there is no lower bound for $M_\Omega = 1, 2, 5, 10$ and we could obtain points satisfying successful strong thermal leptogenesis with arbitrarily small m_1.

However, the fact that $K_{1\mu}^{0,\mathrm{max}}$ is just slightly higher than $K_{\mathrm{st}}(N_{\Delta_\mu})$ (this time $K_{1\mu}^{0,\mathrm{max}} \simeq 11\,M_\Omega$) still implies that one has to fine tune the parameters in the orthogonal matrix in order to maximise $K_{1\mu}$, and this still acts in a way that in the limit $m_1/m_{\mathrm{atm}} \to 0$ the density of points drops quickly. For example one can see that for $M_\Omega = 2$ one still has that 99% of the solutions are found for values $m_1 \gtrsim 3\,\mathrm{meV}$ (the value quoted in the abstract).

---

[8]As a technical detail it is probably worth to stress that for the first time we have randomly generated complex orthogonal matrices (about 10 million of points for both parameterisations) within the whole 6-dim parameter space, without any restriction (except for the bound $|\Omega_{ij}^2| < M_\Omega$).
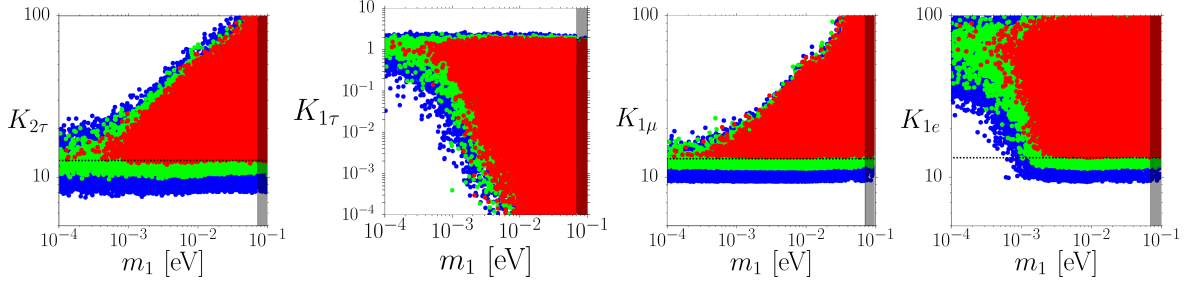
Figure 6. IO case. Results of the scatter plots for $M_\Omega = 2$ for the four relevant flavoured decay parameters $K_{2\tau}, K_{1\tau}, K_{1\mu}, K_{1e}$ versus m_1 (same conventions as in figure 1). The horizontal dotted line indicate $K_{\rm st}(\Delta N_{\Delta\alpha}^{\rm p,i} = 0.03)$.
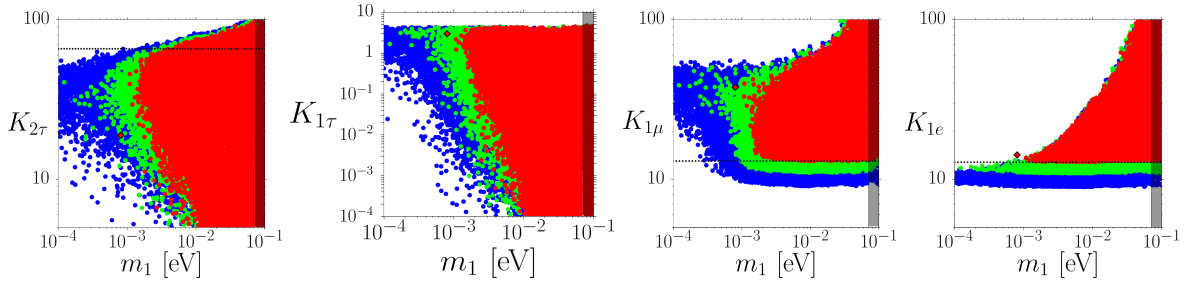

Figure 7. NO case with $M_3 \lesssim 5 \times 10^{11}\,{\rm GeV}$. Results of the scatter plots for $M_\Omega = 2$ for the four relevant flavoured decay parameters $K_{2\tau}, K_{1\tau}, K_{1\mu}, K_{1e}$ versus m_1 (same conventions as in figure 1). The horizontal dotted line indicate $K_{\rm st}(N_{\Delta\alpha}^{\rm p,i} = 0.03)$.

In figure 6 we also show again the results of the scatter plots in the planes $K_{1\alpha} - m_1$ ($\alpha = e, \mu, \tau$). One can see how, while values of $K_{1e} \gg K_{\rm st} \sim 10 - 13$ can be found for arbitrarily small values of m_1, the maximum value of $K_{1\mu}$ for small values of $m_1 \ll m_{\rm atm}$ is just slightly greater than $K_{\rm st}$. This confirms that $K_{1\mu}$ is the crucial quantity that constrains m_1 in the case of IO, since the orthogonal matrix has to be strongly fine tuned in order to have $K_{1\mu} \gtrsim K_{\rm st}$.

4.2 Case $M_3 \lesssim 5 \times 10^{11}\,{\rm GeV}$

As pointed out in 3.2, for $M_3 \lesssim 5 \times 10^{11}\,{\rm GeV}$, the condition $K_{2\tau} \gtrsim K_{\rm st}(N_{\Delta_\tau}^{\rm p,i}) \gg 1$ gets relaxed into $K_{2\tau} + K_{3\tau} \gg K_{\rm st}(N_{\Delta_\tau}^{\rm p,i})$. Potentially this condition can be much more easily satisfied and in particular the value of $K_{2\tau}$ has not to be necessarily very large. In this way the condition of successful leptogenesis becomes independent of the value of the initial pre-existing asymmetry and can be more easily satisfied.

However, this point does not substantially change the results on the absolute neutrino mass scale obtained for the case of large M_3. The reason is that these, as we have seen, depend only on the the $K_{1\alpha}$'s rather than on $K_{2\tau}$ and in particular on the fact that for the NO (IO) case the value of $K_{1e}^{0,\max}$ ($K_{1\mu}^{0,\max}$) is very close to $K_{\rm st}$. In figure 7 we show again $K_{2\tau}$ and the three $K_{1\alpha}$ for the NO case. One can compare the results with those obtained for the case of large M_3 shown in figure 3 and notice how except for $K_{2\tau}$, that now can also be below $K_{\rm st}$, the scatter plot for K_{1e}, the crucial quantity, is substantially the same.

4.3 A few comments on the results

Let us discuss a few points before concluding this section.

The results depend on neutrino oscillation experimental data.   It should be noticed how the results we obtained rely on the smallness of $K_{1e}^{0,\max}$ ($K_{1\mu}^{0,\max}$) for NO (IO) for $K_{1\tau} \lesssim 1$ and this is enforced by the current measured value of the PMNS matrix entries as we have seen, in particular $|U_{e3}|^2 \ll 1$ for NO and $|U_{\mu3} - U_{\tau2}\,U_{\mu3}/U_{\tau3}|^2 \ll 1$ for IO. Therefore, the strong thermal leptogenesis condition realises an interesting interplay between low energy neutrino data and leptogenesis predictions.

Theoretical uncertainties.   Our results have been derived using the analytical expressions eqs. (3.6), (3.10) and (3.12). We have already noticed how these can be derived in the appropriate limit from density matrix equations. Our results neglect momentum dependence in the wash-out but it has been noticed that in the case of strong wash-out, as imposed by strong thermal leptogenesis, this approximation underestimates the wash-out [47] though it has been recently claimed that this is actually an effect that arises not from momentum dependence but from a proper account of quantum statistics in the wash-out rates that increase them by 20% [48]. This would tend to slightly relax our lower bound. On the other hand, taking into account Higgs and quarks asymmetries, would act in the opposite direction [37]. Another consequence of accounting for these asymmetries is flavour coupling. This would tend to open new ways to the pre-existing asymmetry to escape the lightest RH neutrino wash-out [37]. Account of flavour coupling would then act into the direction of tightening the lower bound and this is likely the strongest effect. These effects will be taken into account in a forthcoming publication.

Case $\Delta p_{\mathrm{p}\alpha} = 0$.   How do the results change if the pre-existing asymmetry is assumed to have same flavour composition for leptons and anti-leptons, so that $\Delta p_{\mathrm{p}\alpha} = 0$ in the eqs. (3.10), (3.12)? In this case there is no lower bound for any value of M_Ω, simply because now the strong thermal condition is also satisfied if $\left(1 - p_{e\tau_2^\perp}^0\right) \lesssim 10^{-7}$, independently of the value of K_{1e} depending on m_1. However, it is clear that this possibility is realised for very special models where basically the N_2's have to decay into leptons without a muon component, i.e. $K_{2\mu} = 0$, a very special case though not excluded by experimental data. Indeed in the scatter plots we find a few of such points independently of m_1. However, even though they evade the lower bound on m_1, they basically do not modify the m_1 distributions. Therefore, this caveat corresponds to a very special and definite situation that does not change the general results.

SO(10)-inspired models.   Our results are in perfect agreement with the results found in [43] where, in addition to the strong thermal condition, SO(10)-inspired conditions are also imposed on the Dirac neutrino mass matrix. In this case NO case is a necessary condition. Moreover one finds $M_\Omega \lesssim 0.8$ and our lower bound gives $m_1 \gtrsim 10\,\mathrm{meV}$ that is indeed respected since the range $m_1 = (15\text{–}25)\,\mathrm{meV}$ is found, showing that the SO(10)-inspired conditions further restrict m_1 basically pinning down a very narrow range for m_1.

Form-dominance models [49].   In these models each light neutrino mass is inversely proportional to one different RH neutrino mass. They correspond to an orthogonal matrix equal to one of the six permutation matrices [28]. In this situation the needed cancellation in the eq. (4.2), in order to have $K_{1\tau} \lesssim 1$ and at the same time large K_{1e} and $K_{1\mu}$, is impossible.

The only way to have a small $K_{1\tau}$ in these models is to have small m_1 values with $|\Omega_{11}| \simeq 1$ (while necessarily $\Omega_{21}, \Omega_{31} \simeq 0$) but in this case then, as we have seen, one cannot simultaneously satisfy the conditions $K_{1e}, K_{1\mu} \gg 1$. Therefore form-dominance models cannot realise strong thermal leptogenesis. These two examples show how our analytical procedure can be applied to specific models with definite and in general much stronger constraints on m_1.

4.4 Prospects from future experiments

4.4.1 The importance of solving the ambiguity on neutrino mass ordering

As we have seen for NO successful strong thermal leptogenesis favours $m_1 \gtrsim 10\,\mathrm{meV}$ for $M_\Omega \lesssim 2$ and in our scatter plots we found less than 1% of points at lower values. There is even a strict lower bound $m_1 \gtrsim 1\,\mathrm{meV}$ valid for any choice of the orthogonal matrix. For IO the constrains are looser. There is not such a strict lower bound and only for $m_1 \lesssim 3\,\mathrm{meV}$ we found a number of points less than 1%. It is then very important that in the next years neutrino oscillations experiments will be able to solve the ambiguity between NO and IO neutrino masses. If NO will prove to be correct, then strong thermal leptogenesis can be more easily tested since it strongly favours $m_1 \gtrsim 10\,\mathrm{meV}$, values sufficiently large to produce measurable deviations from the full hierarchical case (i.e. semi-hierarchical neutrinos) in cosmological observations.

4.4.2 Cosmological observations

Cosmological observations are sensitive to neutrino masses and are able to place an upper bound, typically quoted on $\sum_i m_i$ (though future observations might become sensitive to the full neutrino spectrum). Future observations could potentially reach a precision of $\delta(\sum_i m_i) \simeq 10\,\mathrm{meV}$ [50]. In the case of NO, assuming that they would be able to measure the hierarchical lower limit finding $\sum_i m_i = (60 \pm 10)\,\mathrm{meV}$, they would be able to place a 2σ upper bound $m_1 \lesssim 10\,\mathrm{meV}$. From our results this means that future cosmological observations will be potentially able to severely constrain strong thermal leptogenesis with hierarchical RH neutrinos. On the other hand a measurement $\sum_i m_i \gtrsim (95 \pm 10)\,\mathrm{meV}$ would correspond to $m_1 \gtrsim (20 \pm 5)\,\mathrm{meV}$, allowing to place a $2\,\sigma$ lower bound $m_1 \gtrsim 10\,\mathrm{meV}$, and this would be in agreement with the expectations from strong thermal leptogenesis. In the case of IO, a measurement $\sum_i m_i = (100 \pm 10)\,\mathrm{meV}$, in agreement with the hierarchical limit for IO, would correspond to a 2σ upper bound $m_1 \lesssim 15\,\mathrm{meV}$, representing a much looser constraint on strong thermal leptogenesis that in the NO case. Moreover expected values $m_1 \gtrsim 3\,\mathrm{meV}$ would correspond to measurements $\sum_i m_i \gtrsim (100 \pm 10)\,\mathrm{meV}$, in general not distinguishable from the inverted hierarchical limit, i.e. not testable. This shows how NO would be a much more favourable option than IO for a significant test (negative or positive) of strong thermal leptogenesis, since it more strongly favours detectable deviations from the hierarchical limit ($m_1 \to 0$). It should be noticed that NO ordered neutrino masses with $m_1 \simeq 20\,\mathrm{meV}$ would also yield $\sum_i m_i \simeq 100\,\mathrm{meV}$ as for IO hierarchical neutrino masses ($m_1 \ll m_{\mathrm{sol}}$) and this is another reason why it is important that neutrino oscillation experiments will be able to solve the NO-IO ambiguity independently of absolute neutrino mass experiments.

4.4.3 Neutrinoless double beta decay experiments

In the central panel of figure 1 we have also plotted the values of the neutrinoless double beta decay effective neutrino mass m_{ee} versus m_1 from the scatter plot (both for NO and IO). We have also shown the results without imposing strong thermal leptogenesis (yellow points). It

can be seen how for NO, since the effective neutrino mass can be well below m_1 thanks to phase cancellations [51], this can be as small as $\sim 1\,\text{meV}$ even for $m_1 \gtrsim 10\,\text{meV}$ (as indicated by the horizontal and vertical solid lines respectively). This implies that strong thermal leptogenesis is not able to produce effective constraints on m_{ee}. Vice-versa, however, a future measurement of $m_{ee} \gtrsim 10\,\text{meV}$ would imply necessarily $m_1 \gtrsim 10\,\text{meV}$ providing an interesting strong support to the strong thermal leptogenesis expectations. For IO, again, the strong thermal prediction hardly produces detectable deviations from the inverted hierarchical limit.

4.4.4   Tritium beta decay experiments

In the case of absence of signal, the KATRIN experiment will be able to place an upper bound onto the effective electron neutrino mass $m_{\nu_e} \lesssim 250\,\text{meV}$ translating into a similar upper bound on m_1. Therefore, it will not be able to place severe constraints on strong thermal leptogenesis. In the PROJECT 8 experimental proposal [52], the energy of electrons emitted in Tritium beta decay is determined from the frequency of cyclotron radiation and the upper bound could be improved to $m_{\nu_e} \lesssim 50\,\text{meV}$. This would translate again into a similar upper bound on m_1, providing a more stringent constraint but still not able to severely corner strong thermal leptogenesis.

5   Conclusions

Thanks to the current measured values of the neutrino mixing angles, and in particular of θ_{13}, the assumption of strong thermal leptogenesis can be tested quite strongly by future cosmological observations, especially in the NO case. If these will be able to place a stringent upper bound on the lightest neutrino mass scale $m_1 \lesssim 10\,\text{meV}$, then they will strongly corner the idea of strong thermal leptogenesis. This will survive only admitting quite a strong fine tuning in the seesaw formula and/or in the flavoured decay parameters. The result would be much stronger for the NO case than the for the IO case. Therefore, it is important that future neutrino oscillation experiments will be able to solve the NO-IO ambiguity. On the other hand a positive measurement $m_1 \gtrsim 10\,\text{meV}$ could be certainly considered as an important experimental information supporting strong thermal leptogenesis. It is then fascinating that, thanks to the forthcoming advance in the determination of neutrino parameters, we will have soon the opportunity to test important theoretical ideas in relation to a fundamental cosmological puzzle such as the observed matter-antimatter asymmetry of the Universe.

References

[1] PLANCK collaboration, P.A.R. Ade et al., *Planck 2013 results. XVI. Cosmological parameters*, arXiv:1303.5076 [INSPIRE].

[2] M. Fukugita and T. Yanagida, *Baryogenesis Without Grand Unification*, *Phys. Lett.* **B 174** (1986) 45 [INSPIRE].

[3] P. Minkowski, $\mu \to e\gamma$ *at a Rate of One Out of* 10^9 *Muon Decays?*, *Phys. Lett.* **B 67** (1977) 421 [INSPIRE].

[4] T. Yanagida, *Horizontal Gauge Symmetry and Masses of Neutrinos*, in *Proceedings of the Workshop on the Unified Theory and Baryon Number in the Universe*, *Prog. Theor. Phys.* **64** (1980) 1103 [KEK report 79–18 (1979)] [INSPIRE].

[5] M. Gell-Mann, P. Ramond, R. Slansky, *Supergravity*, P. van Nieuwenhuizen and D. Freedman eds., North Holland, Amsterdam (1979), pg. 315.

[6] S.L. Glashow, *1979 Cargese Summer Institute on Quarks and Leptons*, M. Levy, J.-L. Basdevant, D. Speiser, J. Weyers, R. Gastmans and M. Jacobs eds., Plenum Press, New York (1980), pg. 687.

[7] R. Barbieri, D.V. Nanopoulos, G. Morchio and F. Strocchi, *Neutrino Masses in Grand Unified Theories*, *Phys. Lett.* **B 90** (1980) 91 [INSPIRE].

[8] R.N. Mohapatra and G. Senjanović, *Neutrino Mass and Spontaneous Parity Violation*, *Phys. Rev. Lett.* **44** (1980) 912 [INSPIRE].

[9] T. Cohen, D.E. Morrissey and A. Pierce, *Electroweak Baryogenesis and Higgs Signatures*, *Phys. Rev.* **D 86** (2012) 013009 [arXiv:1203.2924] [INSPIRE].

[10] D. Curtin, P. Jaiswal and P. Meade, *Excluding Electroweak Baryogenesis in the MSSM*, *JHEP* **08** (2012) 005 [arXiv:1203.2932] [INSPIRE].

[11] M. Carena, G. Nardini, M. Quirós and C.E.M. Wagner, *MSSM Electroweak Baryogenesis and LHC Data*, *JHEP* **02** (2013) 001 [arXiv:1207.6330] [INSPIRE].

[12] For a recent review see S. Blanchet and P. Di Bari, *The minimal scenario of leptogenesis*, *New J. Phys.* **14** (2012) 125012 [arXiv:1211.0512] [INSPIRE].

[13] R. Kallosh, A.D. Linde, D.A. Linde and L. Susskind, *Gravity and global symmetries*, *Phys. Rev.* **D 52** (1995) 912 [hep-th/9502069] [INSPIRE].

[14] H. Davoudiasl, R. Kitano, G.D. Kribs, H. Murayama and P.J. Steinhardt, *Gravitational baryogenesis*, *Phys. Rev. Lett.* **93** (2004) 201301 [hep-ph/0403019] [INSPIRE].

[15] M. Yoshimura, *Unified Gauge Theories and the Baryon Number of the Universe*, *Phys. Rev. Lett.* **41** (1978) 281 [*Erratum ibid.* **42** (1979) 746] [INSPIRE].

[16] S. Dimopoulos and L. Susskind, *On the Baryon Number of the Universe*, *Phys. Rev.* **D 18** (1978) 4500 [INSPIRE].

[17] D. Toussaint, S.B. Treiman, F. Wilczek and A. Zee, *Matter-Antimatter Accounting, Thermodynamics and Black Hole Radiation*, *Phys. Rev.* **D 19** (1979) 1036 [INSPIRE].

[18] E.W. Kolb and S. Wolfram, *Baryon Number Generation in the Early Universe*, *Nucl. Phys.* **B 172** (1980) 224 [*Erratum ibid.* **B 195** (1982) 542] [INSPIRE].

[19] E.W. Kolb, A.D. Linde and A. Riotto, *GUT baryogenesis after preheating*, *Phys. Rev. Lett.* **77** (1996) 4290 [hep-ph/9606260] [INSPIRE].

[20] I. Affleck and M. Dine, *A New Mechanism for Baryogenesis*, *Nucl. Phys.* **B 249** (1985) 361 [INSPIRE].

[21] D.V. Forero, M. Tortola and J.W.F. Valle, *Global status of neutrino oscillation parameters after Neutrino-2012*, *Phys. Rev.* **D 86** (2012) 073012 [arXiv:1205.4018] [INSPIRE].

[22] F. Capozzi, G.L. Fogli, E. Lisi, A. Marrone, D. Montanino and A. Palazzo, *Status of three-neutrino oscillation parameters, circa 2013*, arXiv:1312.2878 [INSPIRE].

[23] M.C. Gonzalez-Garcia, M. Maltoni, J. Salvado and T. Schwetz, *Global fit to three neutrino mixing: critical look at present precision*, *JHEP* **12** (2012) 123 [arXiv:1209.3023] [INSPIRE].

[24] W. Buchmüller, P. Di Bari and M. Plümacher, *The Neutrino mass window for baryogenesis*, *Nucl. Phys.* **B 665** (2003) 445 [hep-ph/0302092] [INSPIRE].

[25] E. Bertuzzo, P. Di Bari and L. Marzola, *The problem of the initial conditions in flavoured leptogenesis and the tauon N_2-dominated scenario*, *Nucl. Phys.* **B 849** (2011) 521 [arXiv:1007.1641] [INSPIRE].

[26] R. Barbieri, P. Creminelli, A. Strumia and N. Tetradis, *Baryogenesis through leptogenesis*, *Nucl. Phys.* **B 575** (2000) 61 [hep-ph/9911315] [INSPIRE].

[27] G. Engelhard, Y. Grossman, E. Nardi and Y. Nir, *The Importance of N_2 leptogenesis*, *Phys. Rev. Lett.* **99** (2007) 081802 [hep-ph/0612187] [INSPIRE].

[28] P. Di Bari, *Seesaw geometry and leptogenesis*, *Nucl. Phys.* **B 727** (2005) 318 [hep-ph/0502082] [INSPIRE].

[29] A. Abada, S. Davidson, F.-X. Josse-Michaux, M. Losada and A. Riotto, *Flavor issues in leptogenesis*, *JCAP* **04** (2006) 004 [hep-ph/0601083] [INSPIRE].

[30] S. Blanchet, P. Di Bari and G.G. Raffelt, *Quantum Zeno effect and the impact of flavor in leptogenesis*, *JCAP* **03** (2007) 012 [hep-ph/0611337] [INSPIRE].

[31] A. De Simone and A. Riotto, *On the impact of flavour oscillations in leptogenesis*, *JCAP* **02** (2007) 005 [hep-ph/0611357] [INSPIRE].

[32] M. Beneke, B. Garbrecht, C. Fidler, M. Herranen and P. Schwaller, *Flavoured Leptogenesis in the CTP Formalism*, *Nucl. Phys.* **B 843** (2011) 177 [arXiv:1007.4783] [INSPIRE].

[33] B. Garbrecht, F. Glowna and P. Schwaller, *Scattering Rates For Leptogenesis: Damping of Lepton Flavour Coherence and Production of Singlet Neutrinos*, *Nucl. Phys.* **B 877** (2013) 1 [arXiv:1303.5498] [INSPIRE].

[34] O. Vives, *Flavor dependence of CP asymmetries and thermal leptogenesis with strong right-handed neutrino mass hierarchy*, *Phys. Rev.* **D 73** (2006) 073006 [hep-ph/0512160] [INSPIRE].

[35] S. Blanchet and P. Di Bari, *New aspects of leptogenesis bounds*, *Nucl. Phys.* **B 807** (2009) 155 [arXiv:0807.0743] [INSPIRE].

[36] P. Di Bari and A. Riotto, *Successful type-I Leptogenesis with* SO(10)-*inspired mass relations*, *Phys. Lett.* **B 671** (2009) 462 [arXiv:0809.2285] [INSPIRE].

[37] S. Antusch, P. Di Bari, D.A. Jones and S.F. King, *A fuller flavour treatment of N_2-dominated leptogenesis*, *Nucl. Phys.* **B 856** (2012) 180 [arXiv:1003.5132] [INSPIRE].

[38] S. Blanchet, P. Di Bari, D.A. Jones and L. Marzola, *Leptogenesis with heavy neutrino flavours: from density matrix to Boltzmann equations*, *JCAP* **01** (2013) 041 [arXiv:1112.4528] [INSPIRE].

[39] W. Buchmüller, P. Di Bari and M. Plümacher, *Leptogenesis for pedestrians*, *Annals Phys.* **315** (2005) 305 [hep-ph/0401240] [INSPIRE].

[40] S. Blanchet and P. Di Bari, *Flavor effects on leptogenesis predictions*, *JCAP* **03** (2007) 018 [hep-ph/0607330] [INSPIRE].

[41] L. Covi, E. Roulet and F. Vissani, *CP violating decays in leptogenesis scenarios*, *Phys. Lett.* **B 384** (1996) 169 [hep-ph/9605319] [INSPIRE].

[42] J.A. Casas and A. Ibarra, *Oscillating neutrinos and $\mu \to e, \gamma$*, *Nucl. Phys.* **B 618** (2001) 171 [hep-ph/0103065] [INSPIRE].

[43] P. Di Bari and L. Marzola, *SO(10)-inspired solution to the problem of the initial conditions in leptogenesis*, *Nucl. Phys.* **B 877** (2013) 719 [arXiv:1308.1107] [INSPIRE].

[44] S. Antusch, P. Di Bari, D.A. Jones and S.F. King, *Leptogenesis in the Two Right-Handed Neutrino Model Revisited*, *Phys. Rev.* **D 86** (2012) 023516 [arXiv:1107.6002] [INSPIRE].

[45] T. Hambye, Y. Lin, A. Notari, M. Papucci and A. Strumia, *Constraints on neutrino masses from leptogenesis models*, *Nucl. Phys.* **B 695** (2004) 169 [hep-ph/0312203] [INSPIRE].

[46] S. Blanchet and P. Di Bari, *New aspects of leptogenesis bounds*, *Nucl. Phys.* **B 807** (2009) 155 [arXiv:0807.0743] [INSPIRE].

[47] J. Garayoa, S. Pastor, T. Pinto, N. Rius and O. Vives, *On the full Boltzmann equations for Leptogenesis*, *JCAP* **09** (2009) 035 [arXiv:0905.4834] [INSPIRE].

[48] D. Bödeker and M. Wörmann, *Non-relativistic leptogenesis*, *JCAP* **02** (2014) 016 [arXiv:1311.2593] [INSPIRE].

[49] M.-C. Chen and S.F. King, A_4 *See-Saw Models and Form Dominance*, *JHEP* **06** (2009) 072 [arXiv:0903.0125] [INSPIRE].

[50] J. Hamann, S. Hannestad and Y.Y.Y. Wong, *Measuring neutrino masses with a future galaxy survey*, *JCAP* **11** (2012) 052 [arXiv:1209.1043] [INSPIRE].

[51] W. Rodejohann, *Neutrino-less Double Beta Decay and Particle Physics*, *Int. J. Mod. Phys.* **E 20** (2011) 1833 [arXiv:1106.1334] [INSPIRE].

[52] PROJECT 8 collaboration, P.J. Doe et al., *Project 8: Determining neutrino mass from tritium beta decay using a frequency-based method*, arXiv:1309.7093 [INSPIRE].